Performance Analysis of Adaptive Interleaving for OFDM Systems

Sai-Weng Lei and Vincent K. N. Lau

***Abstract*—We proposed a novel interleaving technique for orthogonal frequency division multiplexing (OFDM), namely *adaptive interleaving*, which can break the bursty channel errors more effectively than traditional block interleaving. The technique rearranges the symbols according to instantaneous channel state information of the OFDM subcarriers so as to reduce or minimize the bit error rate (BER) of each OFDM frame. It is well suited to OFDM systems because the channel state information (CSI) values of the whole frame could be estimated at once when transmitted symbols are framed in the frequency dimension. Extensive simulations show that the proposed scheme can greatly improve the performance of the coded modulation systems utilizing block interleaving. Furthermore, we show that the adaptive interleaving out performs any other static interleaving schemes, even in the fast fading channel (with independent fading between symbols). We derived a semi-analytical bound for the BER of the adaptive interleaving scheme under correlated Rayleigh fading channels. Furthermore, we discussed the transmitter–receiver (interleaving pattern) synchronization problem.**

***Index Terms*—Adaptive interleaving, orthogonal frequency division multiplexing (OFDM).**

I. Introduction

On mobile radio channels system performance for high bit rate transmission is often limited by severe intersymbols interference (ISI) resulting from the frequency selective fading of the dispersive channel. Orthogonal frequency division multiplexing (OFDM) is one of the techniques to combat this adverse channel [1], [2]. In OFDM, the information to be transmitted is split over a large number of subcarriers and transmitted in parallel, thus increasing the symbol duration. Each subcarrier will then experience only flat fading and the ISI can be avoided by inserting a guard interval, which is greater than the delay spread of the channel.

On the other hand, error correction codes are usually applied to protect digital source data across the hostile mobile wireless channel. Most of the error correction codes are designed to correct random channel errors [3]. However, channel errors caused by the mobile wireless channel are bursty in nature. Hence, interleaving is usually employed to randomize the bursty channel errors so that error correction codes could be more effective. Traditionally, block interleaving is employed and is shown to be effective in many circumstances.

In this paper, we proposed, for the first time, a novel interleaving technique called *adaptive interleaving* for OFDM systems. This scheme could better exploit the instantaneous channel variation by rearranging the transmitted symbols according to the channel state information (CSI) of the frame. The objective is to break up a long burst of the bad CSI sequence so that the overall bit error probability is reduced or minimized. The proposed adaptive interleaving is well suited for OFDM systems because the transmitted symbols are framed in the frequency dimension and, therefore, the CSI values for the whole frame can be estimated at the same instant.

The potential performance gain for different bandwidth efficiency binary, quadrature, and eight phase-shift keying (BPSK, QPSK, 8PSK) is investigated. Extensive simulation shows that significant E_b/N_0 gain can be obtained with the proposed technique relative to the traditional block interleaving. A semi-analytical bound is derived for the case of correlated Rayleigh fading as a verification to the simulation result.

In general, the proposed adaptive interleaving system would face an important practical problem-pattern synchronization, i.e., both the transmitter and receiver need to use the same permutation to interleave and deinterleave the symbols. A loss of synchronization would be disastrous to the system performance because the receiver would not be able to use the correct permutation to deinterleave and decode a frame. This would most likely cause a lot of errors. Thus, a reliable synchronization mechanism, which can ensure a reasonably low lost-sync rate, is crucial to the adaptive system. For multiframe adaptation, pattern synchronization could easily be achieved by embedding a control header to indicate the transmission permutation (interleaving pattern). This refers to the *closed-loop* approach. However, for fast adaptation, such a closed-loop approach no longer works due to the huge overheads. Therefore, we propose a *quasi-closed-loop* approach that could be applied to fast adaptive interleaving system with minimal overheads.

This paper is organized as follows. Section II describes the system model. In Section III, we discuss the idea of adaptive interleaving. The calculation of the bit error rate (BER) bound is presented in Section IV. The pattern synchronization problem is addressed in Section V. Simulation results to the cases of mobile radio channel are illustrated in Section VI. Finally, we conclude the paper in Section VII.

II. System Model

The system model is depicted in Fig. 1. The input bit streams are first divided into frames, convolutionally coded, and then mapped into symbols. The symbols are then interleaved and modulated by inverse fast Fourier transform (IFFT). After adding cyclic prefix, the OFDM symbols are then transmitted

Manuscript received September 6, 2000; revised April 23, 2001.

This work is supported by CRCG of The University of Hong Kong and the RGC of Hong Kong.

The authors are with the Department of Electrical and Electronic Engineering, University of Hong Kong, Hong Kong (e-mail: swlei@eee.hku.hk; knlau@eee.hku.hk).

Publisher Item Identifier S 0018-9545(02)04949-6.

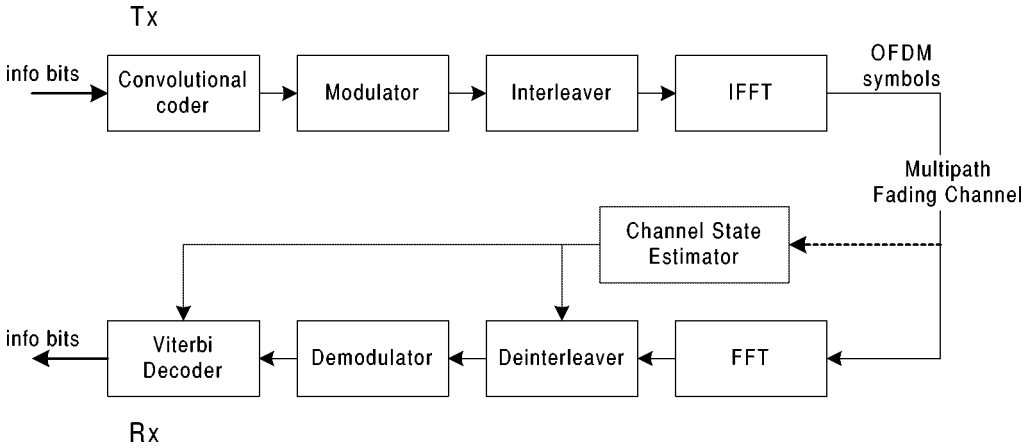

Fig. 1. Block diagram of coded OFDM system.

through a multipath Rayleigh fading channel with N_d discrete paths of equal power.

The received OFDM symbols are then demodulated by using FFT and the demodulated baseband symbol has the form

$$y_m = H_m x_m + n_m \quad m = 1, 2, \ldots, N \tag{1}$$

where x_m ($|x_m| = 1$) is the symbol conveyed by the mth subcarrier, H_m is the corresponding complex frequency gain, and n_m is the complex white Gaussian noise of mean zero and variance N_0/E_s. The complex Gaussian variable H_m has mean zero (Rayleigh distributed fading) and unity variance (channel gain normalized to unity). After deinterleaving, the received symbols are decoded with soft Viterbi decoder. Assuming perfect CSI, maximum likelihood decoding [4] is achieved with the decision metrics given by

$$|y_m - H_m x_m|^2. \tag{2}$$

III. Adaptive Interleaving

The purpose of interleaving is to randomize the bursty channel errors. This can greatly improve the performance of the error-correcting codes, which are often good at correcting random errors. In general, interleaving rearranges the order of symbols to be transmitted according to a given rule. At the receiver, the reverse rule is used to restore the original sequence.

Generally, interleaving can be described by a $n \times n$ square matrix with only 1s and 0s entry, n being the number of the symbols input to the interleaver at a time. If the input symbols row vector is $\mathbf{a}$, then the interleaved one will be

$$\mathbf{a}' = \mathbf{a}M.$$

Consider an example of nine symbols input to a simple 3×3 block interleaver. The interleaving matrix is

$$M = \begin{bmatrix} 1 & 0 & 0 & 0 & 0 & 0 & 0 & 0 & 0 \\ 0 & 0 & 0 & 1 & 0 & 0 & 0 & 0 & 0 \\ 0 & 0 & 0 & 0 & 0 & 0 & 1 & 0 & 0 \\ 0 & 1 & 0 & 0 & 0 & 0 & 0 & 0 & 0 \\ 0 & 0 & 0 & 0 & 1 & 0 & 0 & 0 & 0 \\ 0 & 0 & 0 & 0 & 0 & 0 & 0 & 1 & 0 \\ 0 & 0 & 1 & 0 & 0 & 0 & 0 & 0 & 0 \\ 0 & 0 & 0 & 0 & 0 & 1 & 0 & 0 & 0 \\ 0 & 0 & 0 & 0 & 0 & 0 & 0 & 0 & 1 \end{bmatrix}.$$

Note that any interleaving matrix has one and only one 1 in each column and each row. Thus, if the input to the interleaver is a sequence of 1–9 in ascending order, then the output will be

$$[1, 4, 7, 2, 5, 8, 3, 6, 9].$$

The interleaving matrix M can be written in a compact form as n ordered pairs

$$\{(1,1), (4,2), (7,3), \ldots, (9,9)\}$$

which indicates the positions of 1s in the matrix. For example, (i, j) means the jth column of the ith row. In other words, (i, j) indicates that the ith symbols will be put in the jth position after interleaving.

Similarly, deinterleaving is the same process which permutates the symbols so that the original sequence is restored. Thus, the deinterleaving matrix D is just the inverse of M. The original sequence is

$$\mathbf{a} = \mathbf{a}'D = \mathbf{a}'M^{-1}.$$

The deinterleaving matrix D can be easily derived from M by reversing each ordered pair (i, j) in M to (j, i), i.e., $D = \{(1,1), (2,4), (3,7), \ldots, (9,9)\}$.

Traditionally, the interleaving matrix is fixed for a given system and does not adapt to the varying channel condition. The reason is that symbols are often grouped into frames in time dimension and we can only estimate the CSI at a given time instant. Lacking the CSI for the whole frame, only simple fixed-rule interleaving can be used.

However, in OFDM systems, symbols to be transmitted are grouped into frames in frequency dimension. The CSI for the whole frame could be estimated at the same time. With the availability of such information, a more intelligent interleaving scheme can be done.

The possibility of a better interleaving scheme when the CSI is available can be illustrated in Fig. 2. For illustration, the channel state is simply divided into two states, “Good” and “Bad.” “Good” corresponds to a low attenuation while “Bad” corresponds to high attenuation or deep fade. Also, it is assumed that half of the channel states considered are “Good” and half of them are “Bad.”

Since channel states are correlated in both time and frequency dimension, consecutive of “Good” or “Bad” is expected in the

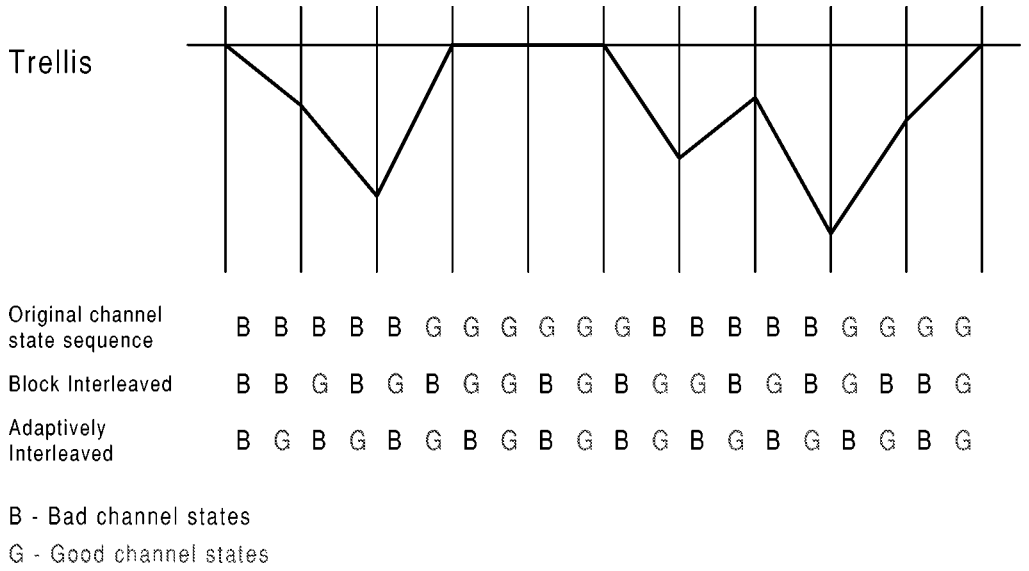

Fig. 2. Block interleaving and adaptive interleaving.

trellis if no interleaving is employed. This is undesirable because the Viterbi algorithm chooses between a correct path and an error path by the accumulated decision metrics covered by the error path. Since the minimum Hamming distance of an error path is $D_{\min}$, a consecutive of $D_{\min}$ or more of "Bad" states will make the decoder very likely to eliminate the correct path, thus contributing an error. Therefore, the criterion is to separate the bursts of "Bad" channel states as far as possible.

After block interleaving, "Bad" and "Good" states become more random and there are less consecutive "Bad" states. Thus, a better BER performance compared with no interleaving can be expected. However, as shown in the figure, there are still some undesirable patterns like "BB" covered by the error paths.

Actually, if the instantaneous channel state sequence is available, a better interleaving scheme is possible. The state could be permutated alternatively with "Bad" and "Good" states, as in Fig. 2. In this way, bursts of "Bad" channel states are completely eliminated from the error path. Therefore, performance gain in error probability could be achieved with this adaptive interleaving scheme compared with block interleaving.

In this paper, we design the adaptive deinterleaver as follows. Fig. 3 shows the process to deduce the deinterleaving pattern. For $k = 1, 2, \ldots, N_f$, let the channel state of the kth subcarrier be H_k and the received symbols be X_k (before deinterleaving). We first sort the symbols in ascending order of the channel state sequence $[|H_i|]_{i=1}^{N_f}$ so that $|H_{k_1}| < |H_{k_2}| < \cdots < |H_{k_{N_f}}|$ and the resulting symbol sequence becomes $[X_{k_1}, X_{k_2}, \ldots, X_{k_{N_f}}]$. The sorted symbols X_{k_i} are then put into a $4 \times (N_f/4)$ matrix as follows:

$$\begin{bmatrix} X_{k_1} & X_{k_2} & \cdots & X_{k_{N_f/4}} \\ X_{k_{N_f/2}} & X_{k_{N_f/2-1}} & \cdots & X_{k_{N_f/4+1}} \\ X_{k_{N_f/2+1}} & X_{k_{N_f/2+2}} & \cdots & X_{k_{3N_f/4}} \\ X_{k_{N_f}} & X_{k_{N_f-1}} & \cdots & X_{k_{3N_f/4+1}} \end{bmatrix}.$$

Note that the second and the fourth rows are reversed in order. (It can be seen that a matrix of other size such as $8 \times (N_f/8)$ or $2 \times (N_f/2)$ can be employed here. However, after evaluating the performance of different matrix size for our system, we found that the size $4 \times (N_f/4)$ gives us the best histogram in Section IV and, hence, better performance.) The symbols are then taken out column by column to form a sequence

$$\left[X_{p_1}, X_{p_2}, \ldots, X_{p_{N_f}}\right]. \tag{3}$$

Hence, the deinterleaving matrix is given by

$$D = \left\{(1, p_1), (2, p_2), \ldots, \left(N_f, p_{N_f}\right)\right\} \tag{4}$$

where p_i is the index of the ith element in the sequence in (3) and $(p_1, p_2, \ldots, p_{N_f})$ is a permutation of the numbers $1, 2, \ldots, N_f$.

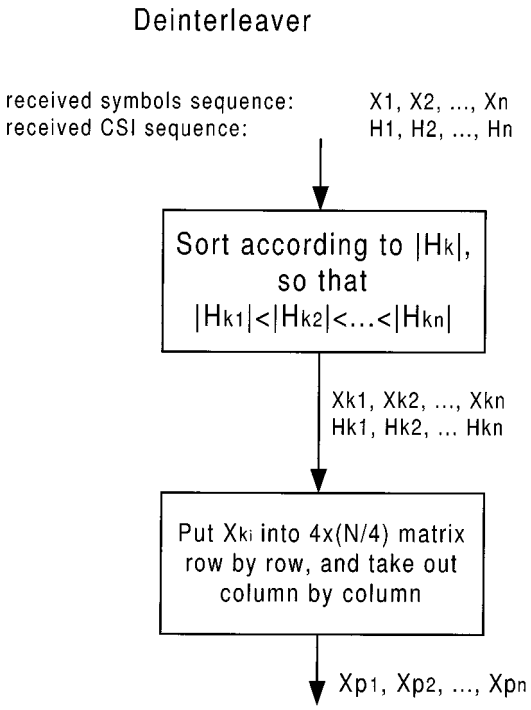

Fig. 3. Deduction of the deinterleaving pattern.

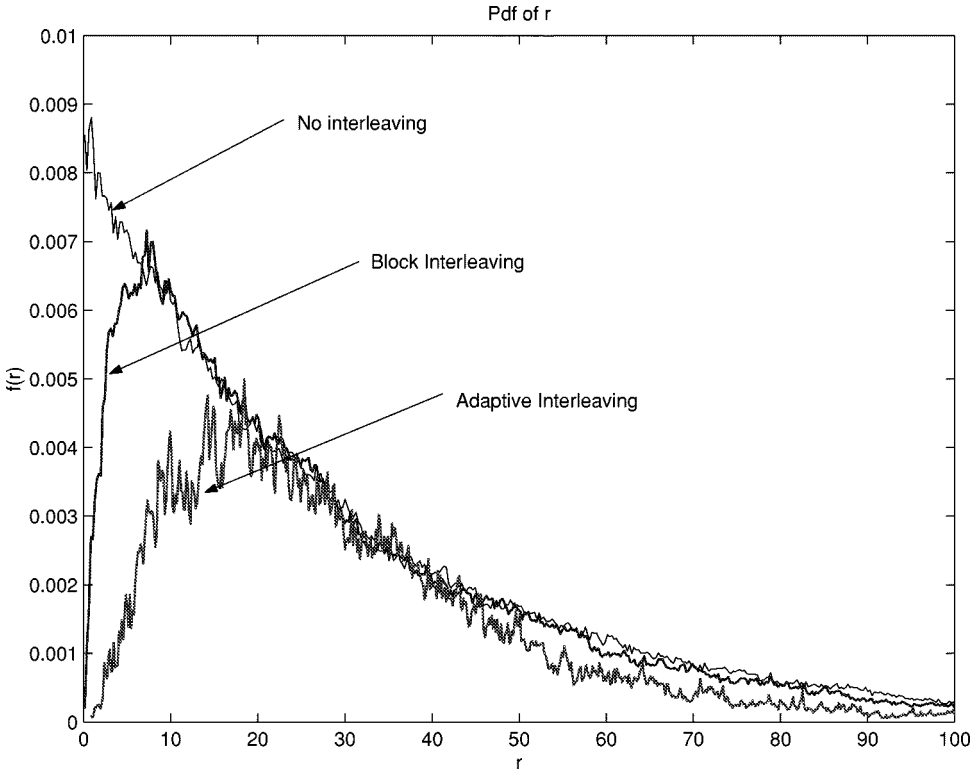

Fig. 4. The pdf of r with different interleaving techniques obtained by simulations.

With the knowledge of the CSI at the transmitter, the same deinterleaving pattern could be obtained and the interleaving matrix for the adaptive interleaver is simply the inverse and is given by

$$I = \left\{(p_1, 1), (p_2, 2), \ldots, \left(p_{N_f}, N_f\right)\right\}. \tag{5}$$

This permutation of the transmitted symbols will result in a more random mix of "Good" and "Bad" states after deinterleaving. Therefore, a gain in performance is expected.

IV. Semi-Analytical Bound of the BER

For a convolutional code of length N, denote the transmitted sequence $(x_1, \ldots, x_N)$ by $\vec{x}$ and the decoded sequence $(t_1, \ldots, t_N)$ by $\vec{t}$. An upper bound on the bit error probability based on the union bound is given by

$$P_b \leq \sum_{\vec{x}, \vec{t} \in C} \sum a(\vec{x}, \vec{t}) P(\vec{x}) P(\vec{x} \to \vec{t}) \tag{6}$$

where $P(\vec{x} \to \vec{t})$ is the pairwise error probability of decoding the sequence $\vec{t}$ instead of the transmitted sequence $\vec{x}$, $P(\vec{x})$ is the probability of transmitting sequence $\vec{x}$, and $a(\vec{x}, \vec{t})$ is the number of erroneous bits between $\vec{x}$ and $\vec{t}$.

By [5], the pairwise error probability conditioned on the fading vector $\vec{\alpha}$ is bounded by

$$P(\vec{x} \to \vec{t} | \, \vec{\alpha}) \leq \prod_{i=1}^{N} e^{-\frac{E_s}{4N_0} |\alpha_i|^2 |x_i - t_i|^2}. \tag{7}$$

Thus, the pairwise error probability can be obtained by averaging (7) over $\vec{\alpha}$.

$$P(\vec{x} \to \vec{t}) \leq \int_{\mathcal{C}^N} P(\vec{x} \to \vec{t} | \, \vec{\alpha}) p(\vec{\alpha}) \, d\vec{\alpha}. \tag{8}$$

For the case of uncorrelated fading (perfect interleaving), the above integral and, thus, P_b can be easily calculated [5]. The result is further extended in [6] to cover the cases of correlated interleaving (partial interleaving). However, the above result cannot be applied to the adaptive interleaving case proposed in this paper. This is because after the channel-state-dependent permutation, the interleaved fading vector $\vec{\alpha}$ is not jointly complex Gaussian as in the partial and perfect interleaving case and the probability density function (pdf) of $\vec{\alpha}$ cannot be expressed in closed form.

Therefore, we would calculate the integral (8) by a numerical method. Substituting (7) into (8), we have

$$P(\vec{x} \to \vec{t}) \leq \int_{\mathcal{C}^N} e^{-\frac{E_s}{4N_0} \sum_{i=1}^{N} |\alpha_i|^2 |x_i - t_i|^2} p(\vec{\alpha}) \, d\vec{\alpha}. \tag{9}$$

The integral is calculated numerically by transforming the N variables α_i into a single scalar

$$r = \sum_{i=1}^{N} |\alpha_i|^2 |x_i - t_i|^2. \tag{10}$$

The probability density function of r pdf $f(r)$ is obtained by simulation. (A large number of frame of size N are generated and the corresponding values of r are calculated and, thus, a histogram of r, which approximates its pdf, could be obtained.) Assume the simulated histogram consists of M bins with bin

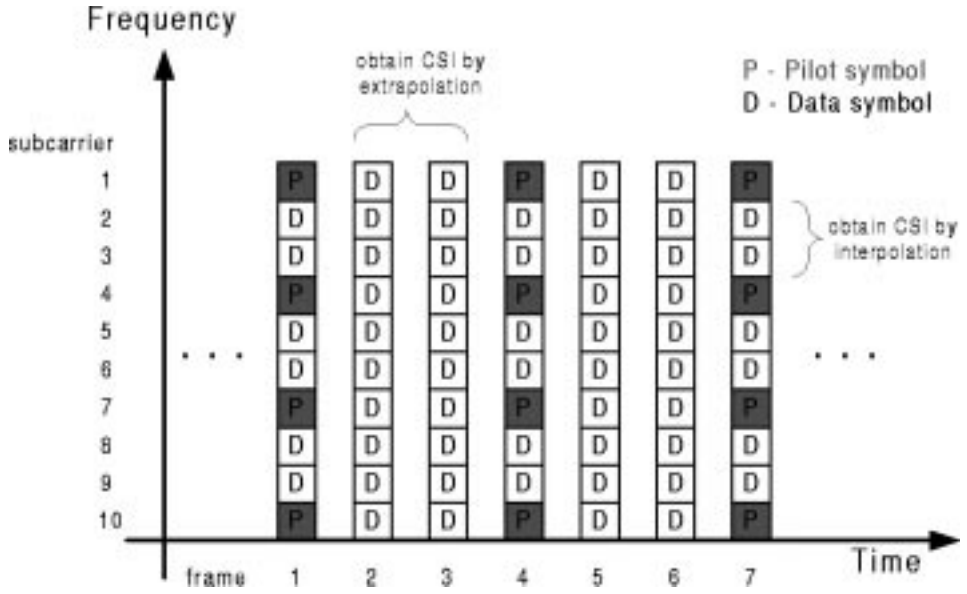

Fig. 5. CSI estimation by inserting grid of pilot symbols.

center $(r_1, \ldots, r_M)$ and $P(r_i)$ denotes the corresponding probability. Then, the numerical integral becomes

$$P(\vec{x} \to \vec{t}) \leq \int_0^\infty e^{-\frac{E_s}{4N_0} r} f(r)\, dr \approx \sum_{i=1}^{M} e^{-\frac{E_s}{4N_0} r_i} P(r_i) \Delta r. \tag{11}$$

As an example, Fig. 4 illustrates the redistribution of the density of r after adaptive interleaving. The channel in this example is modeled as a discrete multipath Rayleigh fading channel with three multipaths of equal power. The convolutional code consists of 1024 symbols. Each frame of 1024 symbols are block interleaved (32×32) and adaptive interleaved (Section III). The interleaved fading vectors are then fed into (10) to calculate r. By generating a large set of such frames and values of r, we obtain the pdf of r ($M = 1000$ bins are used) for different interleaving techniques as in Fig. 4. It can be seen that the probability of small r, which is detrimental to the overall BER, could be reduced through the adaptive interleaving.

V. Practical Considerations: CSI Estimation and Pattern Synchronization

A. CSI Estimation

In order to perform adaptive interleaving, the transmitter has to know the CSI for the current frame. The channel state could be estimated at the receiver with the aid of pilot symbols [7]. Pilot symbols are inserted as shown in Fig. 5 and the CSI of symbols in between pilots are obtained by interpolation.

Since the fading is highly correlated in both time and frequency dimension, the pilot spacing can be large as long as it satisfies the sampling theorem in both dimensions. Therefore, massive feedback of the CSIs can be avoided.

B. Pattern Synchronization

A challenging problem behind the adaptive interleaving systems is to ensure that both the transmitter and receiver are operating at the same permutation. This refers to pattern synchronization.

In the proposed adaptive system, the receiver would estimate the CSI, quantize, error protect them, and then feedback to the transmitter. Based on the feedback of the CSI, the transmitter predicts the future CSIs and then determines the most efficient permutation pattern. The symbols to be transmitted are then interleaved according to the determined pattern and transmitted through the forward channel. Ideally, the receiver could estimate the same CSIs and determine an identical interleaving pattern for deinterleaving. Obviously, a loss of synchronization between would be disastrous to the system performance.

Therefore, a reliable synchronization mechanism, which can ensure a reasonably low lost-sync rate, is crucial to the adaptive system. One trivial method is to embed a control header to indicate the interleaving pattern. This refers to *closed-loop method*. However, it is only feasible for slow adaptation system. For fast adaptation, the huge overhead renders this method useless.

The quasi-closed-loop method is proposed to resolve the problem of huge overhead and also provide a better control between the lost-sync probability and forward control overhead. Actually, in the closed-loop approach, much information embedded in the forward control word is redundant because the receiver already has the copy of the CSIs in the transmitter. Therefore, the receiver can use an identical predictive filter, as in the transmitter. Provided that both the receiver and the transmitter have the same copy of the CSIs sequence, an identical deinterleaving pattern can be obtained at both sides [Fig. 6(a)].

The problem is then down to ensuring an identical set of the CSIs at both the transmitter and the receiver. This is achieved by error protection in feedback channel. As illustrated in Fig. 6(b), at the receiver, the CSI at each pilot position is first quantized and protected separately by adding *cyclic redundancy check* (CRC). At the transmitter, if the feedback CSI is error free, it will be input to the prediction filter. If it is erroneous, it will be ignored and a previous CSI will be input to the filter instead. In the forward channel, the control word is formed by zero or

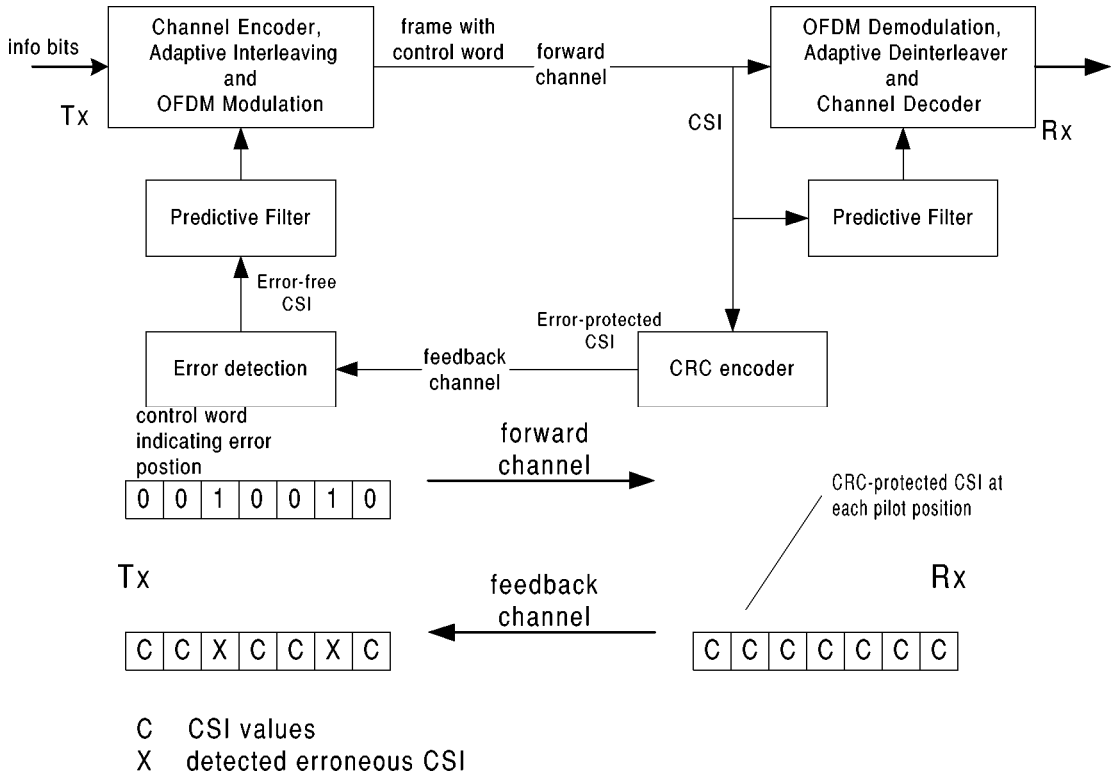

Fig. 6. Pattern synchronization.

one, where one indicates an erroneous CSI and zero indicates an error-free CSI. In this way, the receiver can know which CSIs are ignored and, thus, can synchronize with the transmitter.

VI. Simulation Results and Discussion

Extensive simulations were performed to examine the performance of the adaptive interleaving techniques on a multipath Rayleigh fading channel. The following three coded modulation schemes with different bandwidth efficiency are considered:

1) $1/2$-rate code, BPSK, throughput $= 0.5$;
2) $1/2$-rate code, QPSK, throughput $= 1$;
3) $2/3$-rate code, 8PSK, throughput $= 2$

where the $2/3$-rate code is derived from the $1/2$-rate code by puncturing. The convolutional code used for each scheme are

1) $K = 3, g = (5, 7)$;
2) $K = 5, g = (23, 35)$;
3) $K = 7, g = (133\,171)$

where K is the constraint length, g is the code generator in octal representation, and $D_{\min}$ is the minimum Hamming distance. The channel is a discrete multipath Rayleigh fading channel with N_d path of equal power. The maximum Doppler frequency of the channel is assumed to be 20 Hz (pedestrian speed of 10 km/hr at 2-GHz carrier).

Figs. 7 and 8 show the BER against E_b/N_0 for QPSK and 8PSK modulation, respectively, when constraint length $K = 5$. The frame size is 1024. It is illustrated from the figures that significant E_b/N_0 gain could be achieved by the proposed adaptive interleaving. For example, at BER of 10^{-5}, the adaptive interleaving has E_b/N_0 gain of about 5–7 dB over the traditional block interleaving for different number of multipath ($N_d = 3$ and 9).

The BER plot for $K = 7$ is shown in Fig. 9. A smaller E_b/N_0 gain of 2–3 dB is obtained.

The E_b/N_0 gain of adaptive interleaving over traditional block interleaving at BER of 10^{-5} is summarized in Table I.

It can be observed that the E_b/N_0 gain is much significant for high bandwidth efficiency systems at the same complexity. This is because for high bandwidth efficiency systems, correct path and error path are distinguished by modulation symbols instead of coded bits. Hence, for the same constraint length, the Hamming distance $D_{\min}$ is smaller compared with BPSK systems. Therefore, it is more likely to come across a sequence of bad CSI values. In other words, the potential E_b/N_0 gains for bandwidth efficiency systems are higher. Furthermore, the E_b/N_0 gain decreases as K increases ($D_{\min}$ increases).

Fig. 10 shows the performance of adaptive interleaving for the case of BPSK with $D_{\min} = 9$ and also the BER bound. The bound for the adaptive interleaving is derived by the method proposed in Section IV, while the bounds for no interleaving and block interleaving are calculated based on [5] and [6]. It is shown that the analytical bound of the adaptive interleaving matches the simulated data very well.

Fig. 11 shows the BER against forward E_b/N_0 for different feedback E_b/N_0. The ideal performance of adaptive interleaving is also included in the figure for comparison. In this simulation, the feedback CSI is quantized into 8 bits and then protected by adding 4 bit CRC (CRC generator is $1+D+D^4$). The coded feedback CSI is then BPSK modulated and transmitted. The feedback channel is modeled as Rayleigh fading with Doppler frequency of 20 Hz. A five-order linear

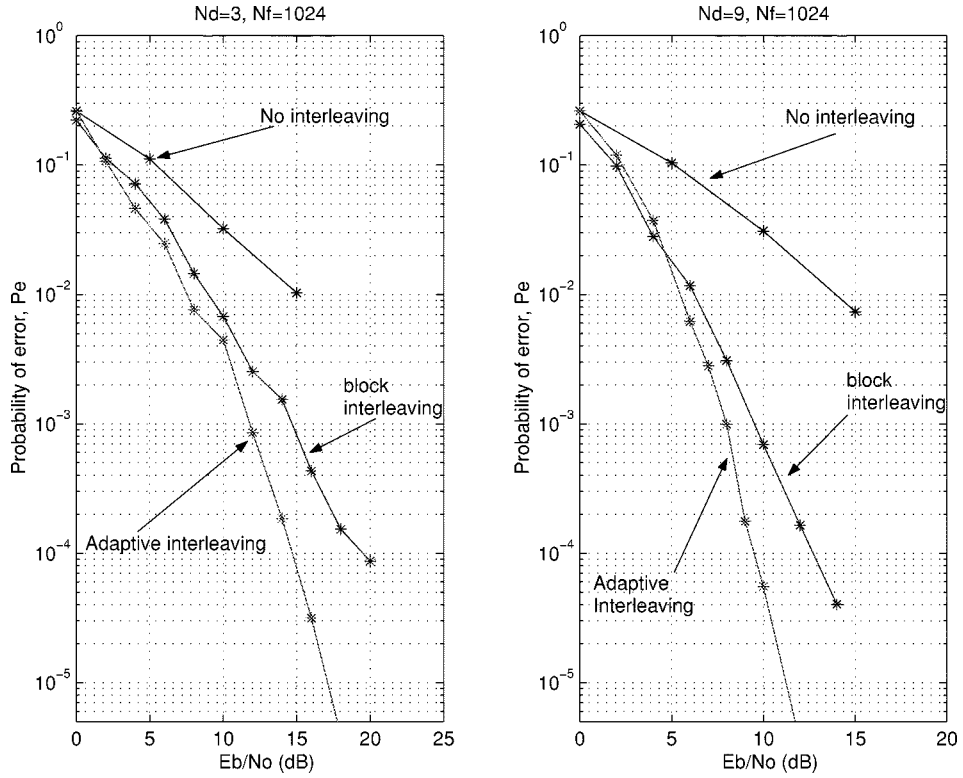

Fig. 7. BER plot for QPSK, $K = 5$.

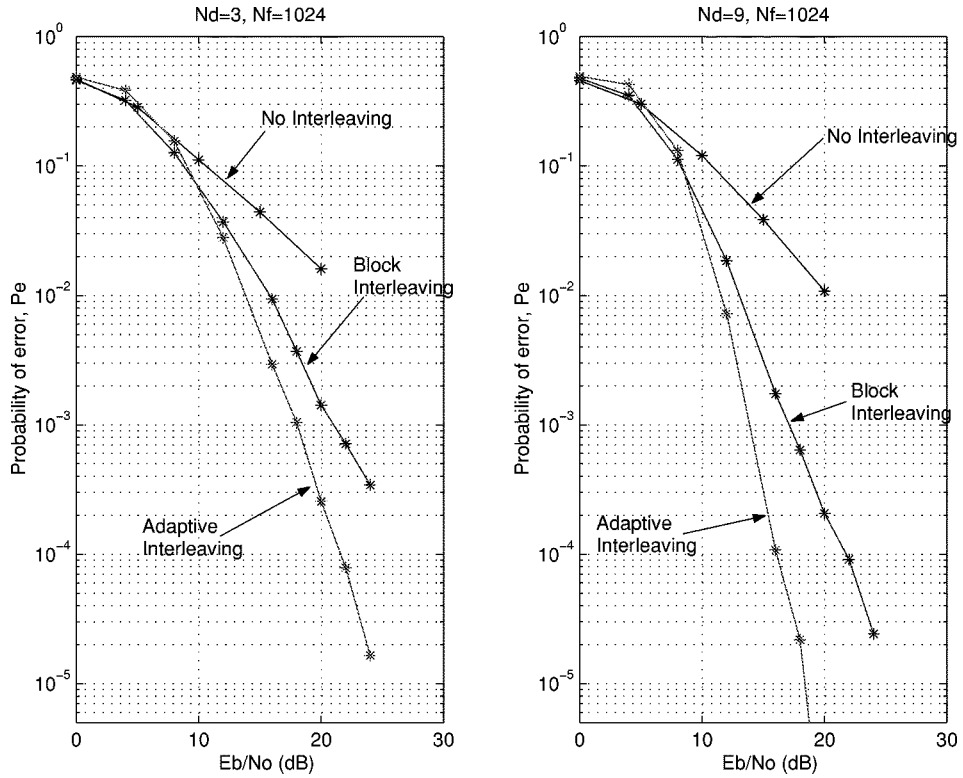

Fig. 8. BER for 8PSK, $K = 5$.

predictive filter is used in both transmitter and receiver to extrapolate the future CSI. The number of subcarriers is 1024 and 12 equally spaced pilot symbols are inserted. The lowpass interpolation Algorithm 8.1 described in [9] is used to obtain the CSI of whole frame.

We can see from the figure that only moderate feedback E_b/N_0 is needed for most operating ranges. (Note that the feedback E_b/N_0 seems large compared with the forward E_b/N_0. However, since the feedback bit rate is much less than the forward one, the required transmitted power of the

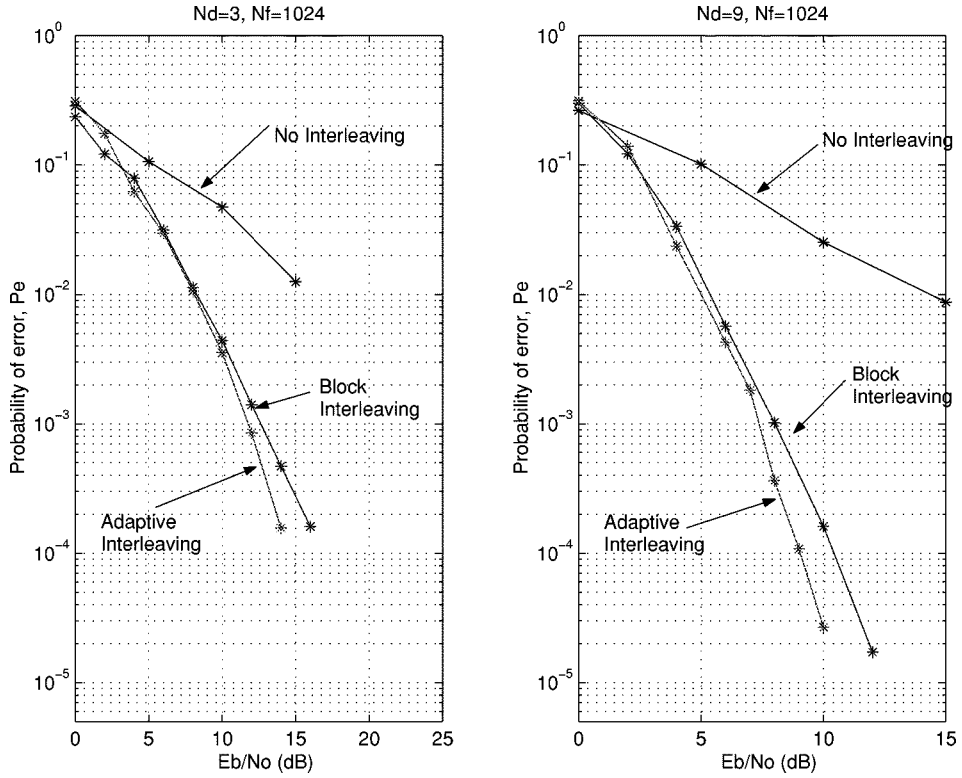

Fig. 9. BER for QPSK, $K = 7$.

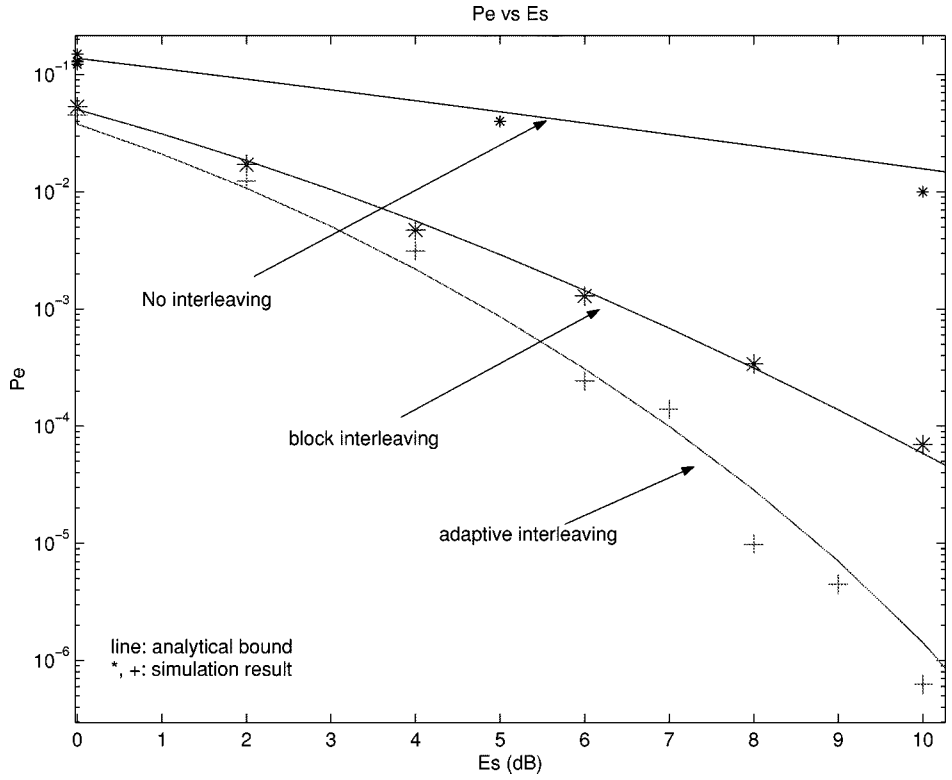

Fig. 10. Semi-analytical bound for the case $D_{\min} = 9$.

feedback channel is even smaller than that of the forward channel.) Furthermore, there is an irreducible error floor when feedback noise is included. This is because the overall BER consists of two parts, the lost-sync rate and the forward error probability, when the system is in sync. At a given feedback E_b/N_0, the BER can be reduced when we boost the forward E_b/N_0. However, at some point of forward E_b/N_0, there will be an irreducible error floor, which is due to the effect of loss

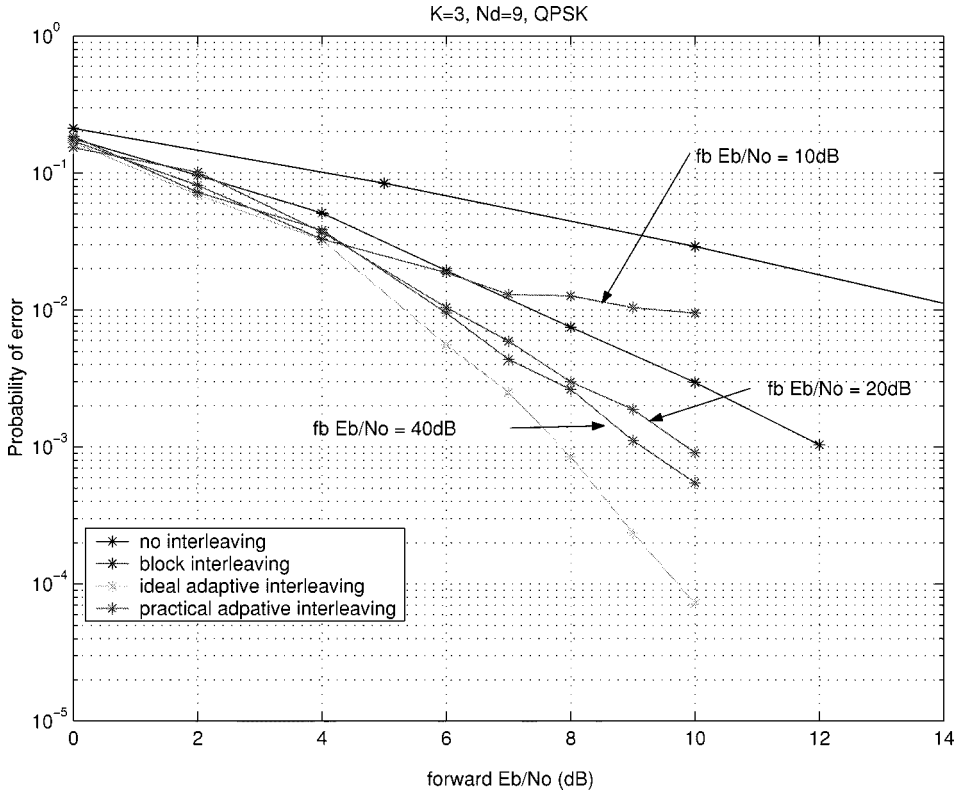

Fig. 11. BER versus *forward* E_b/N_0 with various *feedback* E_b/N_0.

TABLE I
SNR GAINS AT VARIOUS K AND N_d

	N_d	BPSK[8]	QPSK	8PSK
$K=3$	3	5.5dB	8dB	
	9	4.5dB	8.8dB	
$K=5$	3	1.8dB	7.9dB	7.8dB
	9	1.3dB	5dB	7.3dB
$K=7$	3	1.2dB	3dB	
	9	0.4dB	2dB	

of sync. At this time, the bit error is mainly due to loss of synchronization. Thus, further increasing the forward E_b/N_0 makes no difference. This is illustrated in the '$FBE_b/N_0 = 10$ dB' curve in Fig. 11. To reduce the error floor, we have to reduce the lost-sync rate by boosting the feedback E_b/N_0 or by using more powerful error detecting codes, as seen in the curve "$FBE_b/N_0 = 20$ dB" and "$FBE_b/N_0 = 40$ dB."

VII. CONCLUSION

This paper proposes a novel interleaving scheme, namely *adaptive interleaving*, for OFDM systems. This scheme could break long burst of channel error more effectively than traditional block interleaving. Extensive simulations shows that significant E_b/N_0 gain can be obtained, especially in high bandwidth efficiency cases (QPSK and 8PSK). A semi-analytical bound is also derived. The bound is useful for prediction of the performance for a specific scheme and is easy to evaluate. The problem of interleaving pattern synchronization is also taken into account and method for maintaining reliable synchronization between receiver and transmitter is proposed and proved to be effective by simulation.

REFERENCES

[1] B. L. Floch, M. Alard, and C. Berrou, "Coded orthogonal frequency division multiplex," *Proc. IEEE*, vol. 83, pp. 982–996, June 1995.
[2] M. Okada, S. Hara, and N. Morinaga, "Bit error rate performances of orthogonal multicarrier modulation radio transmission systems," *IEICE Trans. Commun.*, vol. E76-B, pp. 113–119, Feb. 1993.
[3] D. J. Costello Jr., J. Hagenauer, H. Imai, and S. Wicker, "Applications of error-control coding," *IEEE Trans. Inform. Theory*, vol. 44, pp. 2531–2560, Oct. 1998.
[4] D. Divsalar and M. K. Simon, "Trellis coded modulation for 4800–9600 bits/s transmission over a fading mobile satellite channel," *IEEE J. Select. Areas Commun.*, vol. SAC-5, pp. 162–175, Feb. 1987.
[5] ——, "The design of trellis coded MPSK for fading channels: Performance criteria—Set partitioning for optimum code design," *IEEE Trans. Commun.*, vol. 36, pp. 1013–1021, Sept. 1988.
[6] K. Leeuwin, J. C. Belfiore, and G. K. Kaleh, "Chernoff bound of trellis-coded modulation over correlated fading channels," *IEEE Trans. Commun.*, vol. 42, pp. 2506–2511, Aug. 1994.
[7] Y. Li, L. J. Cimini Jr., and N. R. Sollenberger, "Robust channel estimation for OFDM systems with rapid dispersive fading channels," *IEEE Trans. Commun.*, vol. 46, pp. 902–915, July 1998.
[8] S. W. Lei, K. N. Lau, and T. S. Ng, Adaptive interleaving for OFDM in TDD systems, in ICC2000, to be published.
[9] Digital Signal Processing Committee, *Programs for Digital Signal Processing*. New York: Wiley, 1979.

Sai-Weng Lei received the B.Eng. degree in electrical and electronic engineering from the University of Hong Kong, Hong Kong, in 1998. He is currently working toward the M.Phil. degree in electrical and electronic engineering at the same University.

His research interests include error-correcting codes, wireless networks, and information theory.

Vincent K. N. Lau received the B.Eng. (distinction first honors) degree from the University of Hong Kong, Hong Kong, in 1992 and the Ph.D. from the University of Cambridge, Cambridge, U.K., in 1997

He joined the HK Telecom, Hong Kong, as System Engineer for three years after graduation and was responsible for transmission systems design. In 1997, he joined Lucent Technologies, Bell Laboratories, Whippany, NJ, as a member of the Technical Staff. He was engaged in the algorithm design, standardization, and prototype development of third generation wide-band code division multiple access (CDMA) systems. He joined the Department of Electrical and Electronic Engineering, Hong Kong University, in 1999 as an Assistant Professor. He was Codirector of the Information Engineering Programme as well as the Codirector of 3G Wireless Technology Center. In July 2001 he left the University and joined the Wireless Advanced Technology Laboratory, Lucent Technology to work on universal mobile telecommunication system (UMTS) and multiple-input multiple-output channel (MIMO) research and development. His research interests includes digital transceiver design, modulation and channel coding, information theory with feedback, power control and CREST factor control algorithms, QoS-based multiple access protocols, and short-range wireless *ad hoc* networking.

Dr. Lau received the Sir Edward Youde Memorial Fellowship from the Croucher Foundation in 1995.